



# OPEN Magnetic properties of polymeric acrylic acid hydrogel dosimeter for radiotherapy applications

Belal Moftah<sup>1,2,4</sup>✉, Khalid A. Rabaeh<sup>3</sup>, Akram A. Moussa<sup>1</sup>, Md Abdullah Al Kafi<sup>1</sup> & Abdullah S. Bani Issa<sup>5</sup>

The present study introduces the first magnetic characterization of a hydrogel dosimeter comprising acrylic acid synthesized within a polyvinyl alcohol matrix. The study aims to accurately assess ionizing radiation dose distributions, making it a valuable tool for radiotherapy treatment. The hydrogel was irradiated to a 1–60 Gy dose range using a medical linear accelerator with dose rates of 100–600 MU/min and radiation beam energies of 6, 10, and 15 MV. The developed dosimeter was synthesized by irradiation-triggered polymerization, and the polymerization degree was indirectly quantified by monitoring the positive alterations in the nuclear magnetic resonance spin–spin relaxation rate. The polymeric hydrogel dosimeter demonstrated an exceptional dose response with an NMR sensitivity of 0.26 Gy<sup>-1</sup>s<sup>-1</sup>, which is 20 times more than the sensitivity of the same gel when measured optically in our previous study. Moreover, it exhibited consistent performance regardless of the beam energy or dose rate.

**Keywords** Radiotherapy, Radiation dosimetry, Quality assurance, Polymer hydrogel, Spectrophotometry, Nuclear magnetic resonance

## Abbreviations

ACA	Acrylic acid
CT	Computed tomography
MRI	Magnetic resonance imaging
NMR	Nuclear magnetic resonance
RT	Room temperature

Hydrogel is a polymeric network in which water serves as the dispersing medium. It has a high degree of elasticity, significant cross-linking in three dimensions (3D), and the ability to expand or contract based on the amount of water in its structure<sup>1</sup>. Hydrogel technology is used in a variety of medical applications, including but not limited to the burn wounds, contact lenses, hyperthermia, controlled drug delivery, and medical radiation dosimetry<sup>2–7</sup>. This study focuses specifically on the latter application, particularly in the context of high-precision radiotherapy techniques. These techniques aim to deliver targeted radiation doses to tumors in three dimensions (3D) while maintaining the integrity of the surrounding healthy tissues<sup>8–12</sup>. Current conventional methods for pretreatment verification to achieve this treatment goal include utilizing 1D dosimeters, such as ion chambers, thermoluminescent detectors, and diode detectors, as well as 2D film dosimeters and 2D ion chambers or diode arrays<sup>13</sup>. However, the low resolution of these 1D or 2D methods tends to induce errors, thereby adding to the uncertain budget of 3D dose distribution evaluations. This highlights the need for a high resolution 3D dosimetry system. Gel dosimeters have emerged as highly effective 3D dosimetry systems with very high resolution for radiotherapy treatment verification<sup>14–19</sup>. They are tissue-equivalent and possess key dosimetric parameters, such as high dose response, wide dose range response linearity, and independence from radiation dose rate, beam energy, and direction<sup>20,21</sup>. Gel dosimeters can be irradiated with different ionizing radiation sources used for various radiotherapy treatment units, and their dose responses can be evaluated by 1D methods, such as spectrophotometry<sup>22,23</sup> and nuclear magnetic resonance (NMR)<sup>24,25</sup>, or in 2D using a charge-coupled

<sup>1</sup>Biomedical Physics Department, King Faisal Specialist Hospital and Research Centre, Riyadh, Saudi Arabia.

<sup>2</sup>Medical and Clinical Affairs, King Faisal Specialist Hospital and Research Centre, Madinah, Saudi Arabia. <sup>3</sup>Medical Imaging Department, Faculty of Applied Medical Sciences, The Hashemite University, Zarqa 13133, Jordan.

<sup>4</sup>Medical Physics Unit, McGill University, Montréal, Canada. <sup>5</sup>Physics Department, Faculty of Science, Yarmouk University, Irbid 21163, Jordan. ✉email: bmoftah@kfshrc.edu.sa

device camera<sup>26</sup>. Polymer gels are mainly characterized by their ability to visualize dose distributions precisely in 3D with optical computed tomography<sup>27–29</sup>, computed tomography (CT)<sup>30,31</sup>, ultraviolet rays<sup>32</sup>, and/or magnetic resonance imaging (MRI)<sup>33–39</sup>. The past few decades have witnessed the widespread utilization of various types of gel dosimeters containing different types of monomers<sup>40–42</sup>. The first polymer gel dosimeter was proposed in 1993<sup>43</sup> and was called an anoxic polymer gel, wherein the deoxygenation process was performed by bubbling the solution with nitrogen gas and acrylamide was used as a monomer, N,N'-methylenediamine-bis-acrylamide (BIS) as a crosslinking agent, and gelatin as a matrix media. After that, various types of gels containing different types of monomers were introduced and evaluated to improve the performance of the original composition<sup>44</sup>.

To reduce the complexity of gel preparation in a nitrogen environment, an advanced composition of polymer gel based on a methacrylic acid monomer was prepared under normal environmental conditions<sup>45</sup>. This type of polymer gel is called a normoxic polymer gel, wherein the deoxygenation process is performed using ascorbic acid as an antioxidant agent. Since then, many research groups have developed various types of normoxic polymer gel dosimeters for dose verification in radiotherapy.

Hayashi et al. (2012)<sup>46</sup> studied the influence of inorganic salts on the dose response of a normoxic methacrylic acid polymer gel dosimeter containing the antioxidant tetrakis (hydroxymethyl) phosphonium chloride (THPC). Changes in the T2 relaxation time of the gels were determined by MRI after irradiation at different doses. They found markedly improved dose sensitivity after increasing salt concentrations from 0 to 1 Molar (M). The authors proposed that the incorporation of inorganic salts into the gel enhances the polymerization rate. This increase in polymerization rate subsequently leads to a higher dose sensitivity of the gel.

Mattea et al. (2015)<sup>47</sup> reported a new polymeric gel dosimeter based on itaconic acid monomers. The gel was irradiated to high doses using dose rates ranging from 158 to 298 cGy/min. The dose response was evaluated using Raman spectroscopy utilizing the changes in chemical differences inside the irradiated gel. Their results showed that the dose response of this type of polymer dosimeter was strongly dependent on the change in the dose rate. A new N-vinylpyrrolidone gel dosimeter with Pluronic F-127 was introduced by Jaszczak and Kozicki (2020)<sup>48</sup>. The gel was irradiated to doses of up to 30 Gy using a medical linear accelerator at different dose rates and beam energies. An NMR relaxometer was used to measure the changes in the R2 relaxation rate of the irradiated gel. They observed that this type of polymer showed approximately 0.19 Gy per second dose sensitivity, a 0–20 Gy linear dose range, and a 1 Gy threshold dose. They also reported that the gel was independent of the type of radiation, dose rate, and beam energy.

Rabaeh et al. (2017)<sup>49</sup> introduced a new normoxic composition of N- (Hydroxymethyl)acrylamide (NHMA) polymer gel dosimeter for radiotherapy applications. After irradiation, the gel was characterized by an NMR relaxometer and an ultraviolet-visible (UV-Vis) spectrophotometer. Although the irradiated NHMA gel demonstrated a good linear dose response of up to 10 Gy in terms of its magnetic and optical properties, it was slightly influenced by variations in dose rate and beam energy. Rabaeh and his group markedly improved the dose sensitivity of the original NHMA composition by adding inorganic salts<sup>50–54</sup>. Recently, Rabaeh et al. (2024)<sup>55</sup>, introduced the first successful acrylic acid (ACA) polymer hydrogel dosimeter. They studied the optical properties of this dosimeter using spectrophotometric technique, and found that the linear dose response extended up to 30 Gy. Additionally, the similar gel was irradiated and scanned by optical computed tomography<sup>56</sup>. The 3D dose map was carried out and compared with the treatment planning system, revealing a slight difference in dose distribution as shown by the gamma pass rate.

This study examined the changes in magnetic properties of the irradiated acrylic acid polymer hydrogel dosimeter which opens the door to measure ionizing radiation dose in three dimensional distributions using nuclear magnetic imaging for radiotherapy treatments. The hydrogel samples were prepared under normal environmental conditions and placed into 10-mm NMR tubes. The irradiated samples were read using the MNR technique, which measures the polymerization degree for different doses in terms of changes in the R2 relaxation rate. While conventional polymer gels melt at room temperature (RT), the ACA hydrogeldosimeter maintains a gelatinous state at this temperature and thus requires no storage in a refrigerator. It also shows high dose sensitivity and a remarkable linear dose response range (up to 30 Gy) with no observable changes in its performance when changing the dose rate or radiation beam energy.

## Materials and methods

The Hydrogel dosimeter was fabricated under normal environmental conditions. Hydrogel composition comprises an ACA monomer, a polyvinyl alcohol (PVA) matrix, a glutaraldehyde (GTA) crosslinking agent, an N, N-methylene- bis-acrylamide (BIS) comonomer, a THPC antioxidant agent, a magnesium chloride (MgCl<sub>2</sub>) inorganic sensitizing agent, and a triple distilled water solvent. Merck Group (St. Louis, Missouri, USA) supplied all high-purity chemicals used for fabrication. The hydrogel gel was prepared as follows: 1 M of MgCl<sub>2</sub> salt was added to triple distilled water at RT and magnetically stirred for approximately 30 min. After increasing the salt solution temperature to 80 °C, 5 wt% PVA powder was added and stirred continuously until a clear solution was obtained. Then, the solution temperature was reduced to approximately 50 °C, 3 wt% BIS powder was added, and the solution was stirred for approximately 1 h. Once the BIS was completely dissolved, the hydrogel solution temperature was lowered to approximately 40 °C, and 0.5 wt% ACA, 0.5 wt% GTA, and 0.3 wt THPC were added one after the other. The mixture was stirred for approximately 4–5 min while each of those chemicals was added. The fabricated hydrogel was then filled directly into airtight 10 ml NMR tubes (Wilma Glass, Buena, NJ, USA). The hydrogel samples were maintained at RT (approximately 22 °C) both before and after irradiation. In contrast, previous types of polymer gel dosimeters typically needed to be refrigerated at 10 °C to transition from a liquid state to a gel state and required continuous storage at low temperatures to prevent melting. Interestingly, our ACA hydrogel polymer dosimeter can transition from a liquid state to a gelatinous state at RT within a few hours after preparation. Furthermore, the shelf life of the ACA hydrogel polymer dosimeter extends to a couple of months upon RT storage in the dark.

The ACA hydrogel samples in the NMR tubes were irradiated a day after gel preparation. To balance the sample temperature with that of the irradiation room, the hydrogel samples were kept in the room for a few hours before irradiation. The samples were then exposed to a dose range of 1–60 Gy using a medical linear accelerator (Varian Medical Systems, Palo Alto, California, USA) with a 6 MV photon beam at a 600 MU/min dose rate. Each hydrogel sample was irradiated in a water phantom ( $30 \times 30 \times 30 \text{ cm}^3$ ) with a  $10 \times 10 \text{ cm}^2$  field size and 100 cm source-to-surface distance at a depth of 5 cm. To study the effect of the dose rate and beam energy on the performance of the ACA hydrogel samples, some samples were irradiated at different dose rates, such as 100, 200, 300, and 400 MU/min, with 6 MV of energy. Other samples were exposed to different radiation beam energies (10 and 15 MV) at 600 MU/min. For each energy and dose rate combination, a set of three samples was used, and the median value of the dose response was recorded for this study. After irradiation, the samples were RT-stored in the dark.

Changes in the magnetic properties of the irradiated ACA hydrogel samples in NMR tubes were assessed in terms of changes in the relaxation rate (R2) using a 0.5 T NMR relaxometer (Minispec mq20, Bruker, Germany). The R2 values were obtained after applying the Multi-Spin- Echo (Carr Purcell Meiboom Gill sequence) with 0.5 ms echo time spacing and 2000 echoes. To reduce the influence of the NMR scanning temperature, a thermostatic circulating water bath (Julabo, Germany) was connected to the NMR relaxometer to control the scanning temperature (approximately  $20 \pm 0.1^\circ \text{C}$ ). The NMR hydrogel samples were placed in a thermostatic circulating water bath 1 h before NMR measurements to allow them to equilibrate to a controlled constant temperature. Three measurements were taken for each MNR sample, and the median value of the measurements was reported in this experiment. A standard NMR sample supplied by Bruker Company was used to calibrate the NMR relaxometer before scanning the hydrogel samples.

## Results and discussion

The dose response and sensitivity of the ACA hydrogel dosimeter were evaluated after irradiating the hydrogels with an absorbed dose range of 1–60 Gy. Figure 1 shows the visual changes in opacity (representing the changes in the R2 relaxation rate) of the unirradiated and irradiated hydrogels for different absorbed doses. The ionizing radiation-induced dissociation of  $\text{H}_2\text{O}$  molecules (which is the major component of the hydrogel,) yields highly reactive species (ions and free radicals). This generated free radical comonomers, which, in turn, initiated the polymerization reaction inside the hydrogel matrix, increasing the optical intensity of the hydrogel and rising the relaxation rates of the water proton surrounding polymer. Consequently, the spin-spin relaxation rate (R2) can be utilized to assess the dose-response. Higher ionizing radiation dose to the hydrogel yielded more polymers (Fig. 1). Therefore, the R2 relaxation rate of the irradiated polymeric hydrogel increased linearly up to 30 Gy, after which the response starts to saturate due to the consumption of comonomers (Fig. 2). All the irradiated gel samples were read using an NMR relaxometer after one-day irradiation for the polymerization to stabilize. The efficiency of the ACA hydrogel samples was obtained from the dose sensitivity, which was calculated from the slope of the linear plot (up to 30 Gy) of the relaxation rate versus the dose (see the inset of Fig. 2). In contrast to the prior study by Rabaeh et al. (2024)<sup>55</sup>, which examined the same gel optically and found a dose sensitivity of  $0.013^{-1} \text{ s}^{-1}$ , the dose sensitivity in this study exceeded  $0.26 \text{ Gy}^{-1} \text{ s}^{-1}$ , surpassing the values published for most conventional polymer dosimeters, such as the NIPAMGAT polymer gel ( $0.12 \text{ Gy}^{-1} \text{ s}^{-1}$ )<sup>57</sup> and the PAGAT polymer gel ( $0.09 \text{ Gy}^{-1} \text{ s}^{-1}$ )<sup>58</sup>, due to higher rate of polymerization reaction of ACA and BIS. Apart

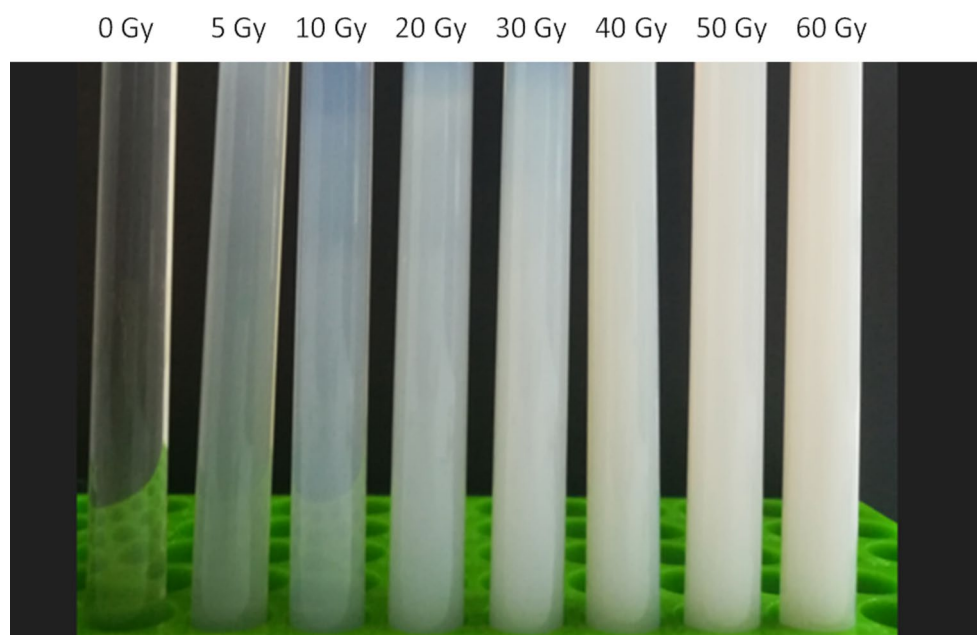


**Fig. 1.** Photograph of unirradiated and irradiated polymeric hydrogel for different absorbed doses.

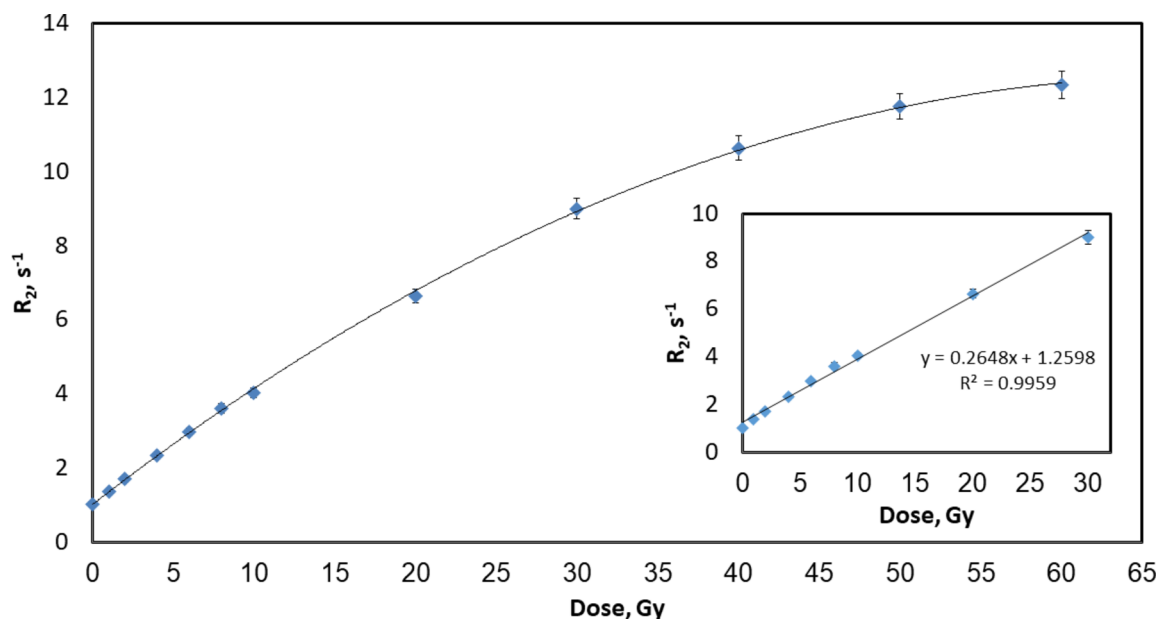


**Fig. 2.** Changes in relaxation rate ( $R_2$ ) of ACA hydrogel polymer gel as a function of absorbed dose.

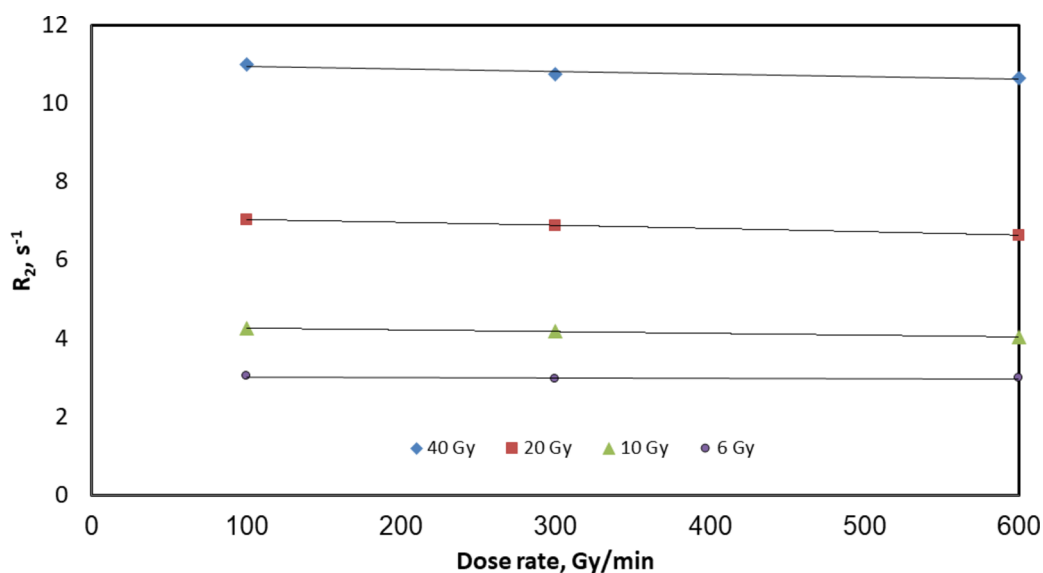


**Fig. 3.** Changes in relaxation rate ( $R_2$ ) of ACA hydrogel as a function of dose rate.

from demonstrating a wider linear range of up to 30 Gy, compared to less than 20 Gy for conventional polymer gels, our dosimeter demonstrated high transparency. This was measured previously<sup>55</sup> as an optical intensity of 0.12 before irradiation (see Fig. 1). In contrast, other polymer gel compositions often lack full transparency, frequently appearing yellow; for instance, the optical intensity of the NMPAGAT polymer gel dosimeter is approximately 0.23<sup>59</sup>. Additionally, this composition can be RT-stored, whereas others must be refrigerated to prevent melting.

The dose rate impact on hydrogel dosimeter performance was investigated at 100–600 MU/min for a fixed radiation beam energy of 6 MV. The samples were irradiated to doses of 6, 10, 20, and 40 Gy under similar exposure conditions used to obtain the results shown in Fig. 2. A set of three hydrogel samples was exposed to each selected dose, and the average dose response in terms of the  $R_2$  relaxation rate or absorbance intensity was recorded (as represented in Fig. 3). The results showed no significant changes in the relaxation rate of the irradiated polymeric hydrogels when the dose rate was varied from 100 to 600 MU/min (maximum coefficient of variation < 0.03). Therefore, this new polymeric hydrogel can be used for quality assurance in medical radiation dosimetry across a range of dose rates, eliminating the need to adjust its response for specific dose rates and thereby enhancing the accuracy of the dosimeter under various clinical conditions.

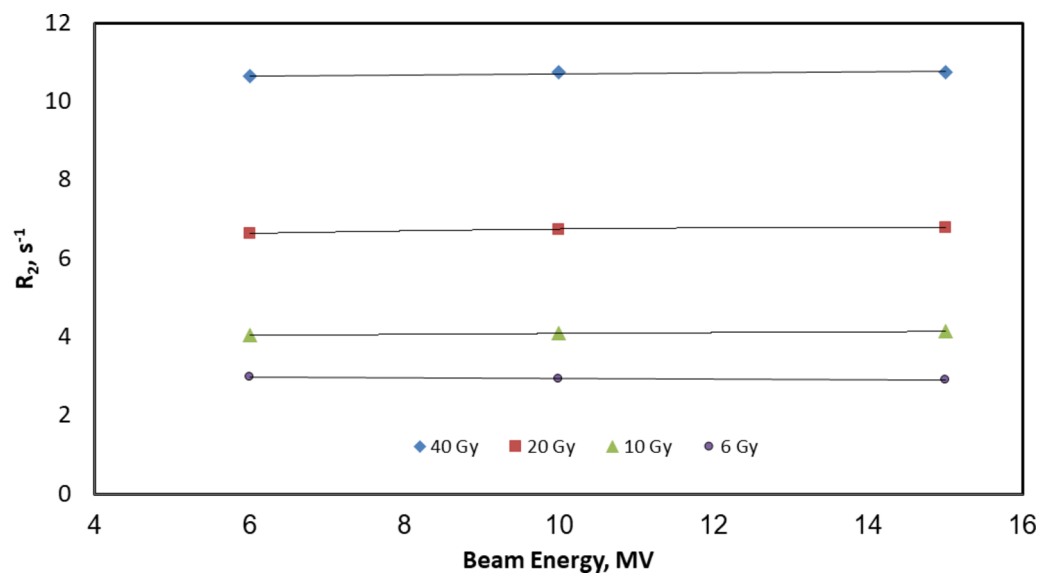


**Fig. 4.** Changes in the relaxation rate ( $R_2$ ) of ACA hydrogel as a function of radiation energy.

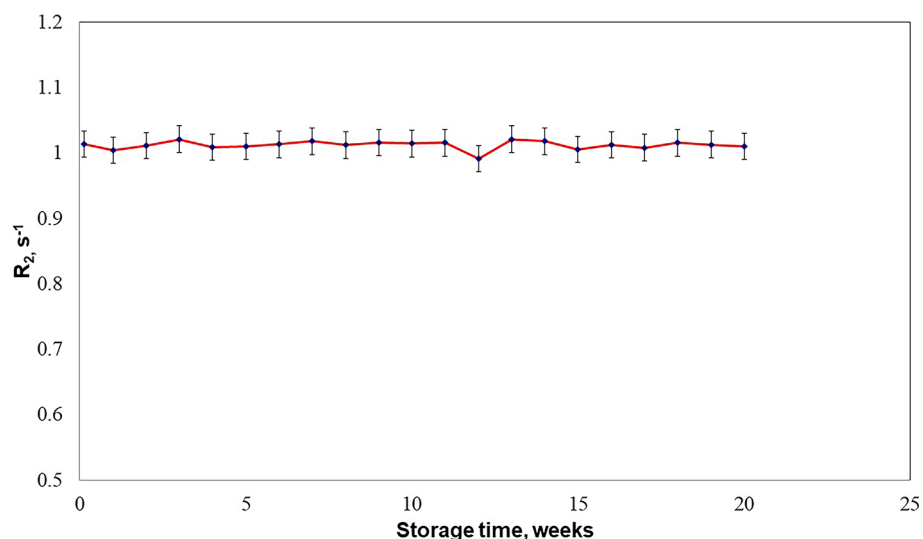


**Fig. 5.**  $R_2$  relaxation rate of unirradiated ACA hydrogel dosimeter as a function of storage time up to 20 weeks.

To investigate the effect of radiation beam energy on the dose response of the ACA hydrogel dosimeter, the most widely used radiation therapy energy range (6–15 MV) was selected with a fixed dose rate of 600 MU/min. The hydrogel dosimeters were exposed to specific doses of 6, 10, 20, and 40 Gy. The maximum coefficient of variation for the relaxation rate (Fig. 4) was approximately 0.012. The observed dose-independent response and dose insensitivity to the megavoltage beam energy enhance the dosimeter's accuracy across various clinical settings. This underscores the feasibility of utilizing the ACA hydrogel dosimeter for routine quality assurance in radiotherapy.

The unirradiated polymeric hydrogel dosimeter samples were read for 20 weeks after preparation on a weekly basis to evaluate the shelf life of the hydrogels. The  $R_2$  relaxation rate of a set of five hydrogel samples was obtained, and the average value was recorded, as reported in Fig. 5. The results show that the unirradiated polymeric hydrogel relaxation rate was almost unchanged with increasing storage time up to 20 weeks, indicating that the prepared new polymeric gel can be RT-stored for a long time without increasing its background temperature or reducing its dose sensitivity. Additionally, the irradiated hydrogel stability was evaluated in this study by irradiating the polymeric hydrogel to various doses and reading its response for up to two weeks. A group of three samples of hydrogel was exposed to each selected dose. Figure 6 depicts the average relaxation rates for each group. The results show that the irradiated hydrogel relaxation rate increases by approximately 25% over a storage time of up to 4 days due to the continuity of the polymerization process. Self-development declines

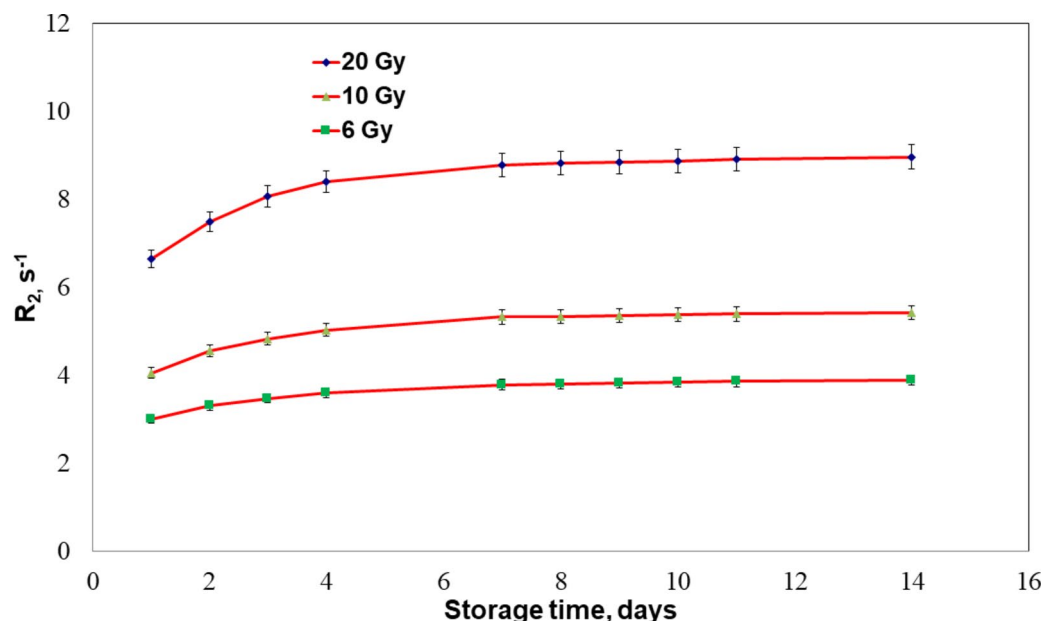


**Fig. 6.**  $R_2$  relaxation rate of ACA hydrogel dosimeter irradiated to 6, 10, and 20 Gy as a function of storage time.

with time and results in a stable dose response beyond 4 days, and the stability extends to 14 days, where the differences in relaxation rate are within the margin of errors. Efforts are ongoing to improve the initial stability of the ACA hydrogel dosimeter relaxation rate for the first 4 days. To achieve optimal post-stability, we recommend evaluating all gel samples under one of the following conditions: (1) after one day and within a few hours post-irradiation, or (2) four days after irradiation.

## Conclusions

An acrylic acid hydrogel dosimeter system containing radiosensitive monomers suitable for quality assurance in medical radiation dosimetry was evaluated using relaxometry technique. The polymeric hydrogel dosimeters contained acrylic acid monomer, which polymerized as the absorbed dose increased to 60 Gy. The developed hydrogels are gelatinous substances that can be RT-stored before and after irradiation, whereas conventional polymer gels must be stored at low temperatures to prevent melting. The dose response of the hydrogel was investigated in terms of changes in the NMR relaxation rate ( $R_2$ ). While the new hydrogel dosimeter had a wider linear dose range (0–30 Gy) than conventional polymer gels with similar dose sensitivities, it exhibited no significant response or dependence on changes in dose rates or beam energies.

## Data availability

Data is provided within the manuscript.

Received: 5 February 2025; Accepted: 27 March 2025

Published online: 16 April 2025

## References

1. Stanciu, L., Diaz-Amaya, S. & Biomaterials, C. *Elsevier eBooks* 149–169. <https://doi.org/10.1016/b978-0-12-809263-7.00007-x>. (2022).
2. Çelik, E. & Akelma, H. Hydrogel burn dressing effectiveness in burn pain. *Burns* **50**, 190–196. <https://doi.org/10.1016/j.burns.2023.08.012> (2024).
3. Ganguly, S. & Margel, S. Design of magnetic hydrogels for hyperthermia and drug delivery. *Polymers* **13** (23), 4259. <https://doi.org/10.3390/polym13234259> (2021).
4. Ganguly, S. & Margel 3D printed magnetic polymer composite hydrogels for hyperthermia and magnetic field driven structural manipulation. *Prog. Polym. Sci.* **131**, 101574. <https://doi.org/10.1016/j.progpolymsci.2022.101574> (2022).
5. Londhe, P. V. et al. Magnetic hydrogel (MagGel): an evolutionary pedestal for anticancer therapy. *Coord. Chem. Rev.* **522**, 216228 (2025).
6. Ganguly, S. et al. Superparamagnetic Amine-Functionalized maghemite nanoparticles as a Thixotropy promoter for hydrogels and magnetic Field-Driven Diffusion-Controlled drug release. *ACS Appl. Nano Mater.* **7** (5), 5272–5286. <https://doi.org/10.1021/acsanm.3c05543> (2024).
7. Moftah, B., Basfar, A. A., Almousa, A. A., Al Kafi, A. M. & Rabaeh, K. A. Novel 3D polymer gel dosimeters based on N-(3-Methoxypropyl)acrylamide (NMPAGAT) for quality assurance in radiation oncology. *Radiat. Meas.* **135**, 106372. <https://doi.org/10.1016/j.radmeas.2020.106372> (2020).
8. Zhang, P., Jiang, L., Chen, H. & Hu, L. Recent advances in hydrogel-based sensors responding to ionizing radiation. *Gels* **8**, 238. <https://doi.org/10.3390/gels8040238> (2022).



9. Abtahi, S. M. M., Anaraki, V., Farhood, B. & Mahdavi, S. R. Assessment of photon energy and dose rate dependence of U-NIPAM polymer gel dosimeter. *Radiat. Phys. Chem.* **172**, 108784. <https://doi.org/10.1016/j.radphyschem.2020.108784> (2020).
10. Massillon-JL, G. Future directions on low-energy radiation dosimetry. *Sci. Rep.* **11**, 10569. <https://doi.org/10.1038/s41598-021-90152-3> (2021).
11. Maeyama, T. et al. Dose-rate-independent and diffusion-free nanoclay-based radio-fluorogenic gel dosimeter. *Sens. Actuators A.* **298**, 111435. <https://doi.org/10.1016/j.sna.2019.06.015> (2019).
12. Farhood, B. et al. Dosimetric characteristics of PASSAG as a new polymer gel dosimeter with negligible toxicity. *Radiat. Phys. Chem.* **147**, 91–100. <https://doi.org/10.1016/j.radphyschem.2018.02.010> (2018).
13. Yasuda, H. & Morioka, S. Comparative study on measurements of radiochromic films using portable colorimeters. *Sci. Rep.* **14**, 3384. <https://doi.org/10.1038/s41598-024-54017-9> (2024).
14. Valente, M. et al. Water-equivalence of gel dosimeters for radiology medical imaging. *Appl. Radiat. Isot.* **141**, 193–198. <https://doi.org/10.1016/j.apradiso.2018.03.005> (2018).
15. Gallo, S. et al. Preliminary magnetic resonance relaxometric analysis of Fricke gel dosimeters produced with Polyvinyl alcohol and glutaraldehyde. *Nucl. Technol. Radiat. Prot.* **32**, 242–249. <https://doi.org/10.2298/NTRP1703242G> (2017).
16. Gallo, S. et al. Does the gelation temperature or the sulfuric acid concentration influence the dosimetric properties of radiochromic PVA-GTA Xylenol orange Fricke gels? *Radiat. Phys. Chem.* **160**, 35–40. <https://doi.org/10.1016/j.radphyschem.2019.03.014> (2019).
17. Gallo, S. et al. Temperature behavior of radiochromic poly(vinyl-alcohol)-glutaraldehyde Fricke gel dosimeters in practice. *J. Phys. D: Appl. Phys.* **53**, 365003. <https://doi.org/10.1088/1361-6463/ab9265> (2020).
18. O'Leary, M. et al. Observation of dose-rate dependence in a Fricke dosimeter irradiated at low dose rates with monoenergetic X-rays. *Sci. Rep.* **8**, 4735. <https://doi.org/10.1038/s41598-018-21813-z> (2018).
19. Baldock, C. et al. Polymer gel dosimetry. *Phys. Med. Biol.* **55**, R1–63. <https://doi.org/10.1088/0031-9155/55/5/R01> (2010).
20. Soliman, Y. S., Beshir, W. B., Abdelgawad, M. H., Bräuer-Krisch, E. & Abdel-Fattah, A. A. Pergascript orange-based polymeric solution as a dosimeter for radiotherapy dosimetric validation. *Phys. Med.* **57**, 169–176. <https://doi.org/10.1016/j.ejmp.2019.01.005> (2019).
21. Soliman, Y. S. Gamma-radiation induced synthesis of silver nanoparticles in gelatin and its application for radiotherapy dose measurements. *Radiat. Phys. Chem.* **102**, 60–67. <https://doi.org/10.1016/j.radphyschem.2014.04.023> (2014).
22. Lotfy, S., Basfar, A. A., Moftah, B. & Al-Moussa, A. A. Comparative study of nuclear magnetic resonance and UV-visible spectroscopy dose-response of polymer gel based on N-(Isobutoxymethyl) acrylamide, nucl. Instrum. *Methods Phys. Res. Sect. B.* **413**, 42–50. <https://doi.org/10.1016/j.nimb.2017.09.033> (2017).
23. Abtahi, S. M., Aghamiri, S. M. R. & Khalafi, H. Optical and MRI investigations of an optimized acrylamide-based polymer gel dosimeter. *J. Radioanal. Nucl. Chem.* **300**, 287–301. <https://doi.org/10.1007/s10967-014-2983-7> (2014).
24. Rabaeh, K. A., Al-Ajaleen, M. S., Abuzayed, M. H., Aldweri, F. M. & Eyadeh, M. M. High dose sensitivity of N-(isobutoxymethyl) acrylamide polymer gel dosimeters with improved monomer solubility using acetone co-solvent. *Nucl. Instrum. Methods Phys. Res., Sect. B.* **442**, 67–72. <https://doi.org/10.1016/j.nimb.2019.01.029> (2019).
25. Basfar, A. A., Moftah, B., Rabaeh, K. A. & Almousa, A. A. Novel composition of polymer gel dosimeters based on N-(Hydroxymethyl) acrylamide for radiation therapy. *Radiat. Phys. Chem.* **112**, 117–120. <https://doi.org/10.1016/j.radphyschem.2015.03.024> (2015).
26. Mariani, M., Vanossi, E., Gambarini, G., Carrara, M. & Valente, M. Preliminary results from a polymer gel dosimeter for absorbed dose imaging in radiotherapy. *Radiat. Phys. Chem.* **76**, 1507–1510. <https://doi.org/10.1016/j.radphyschem.2007.02.080> (2007).
27. Awad, S. I. et al. 3-D quality assurance in cyberknife radiotherapy using A novel N-(3-Methoxypropyl) acrylamide polymer gel dosimeter and optical CT. *Radiat. Phys. Chem.* **161**, 34–41. <https://doi.org/10.1016/j.radphyschem.2019.03.045> (2019).
28. Adliene, D., Jakstas, K. & Vaiciunaite, N. Application of optical methods for dose evaluation in normoxic polyacrylamide gels irradiated at two different geometries. *Nucl. Instrum. Methods Phys. Res. Sect. A.* **741**, 88–94. <https://doi.org/10.1016/j.nima.2013.12.057> (2014).
29. Oldham, M., Siewersden, H. H., Shetty, A. & Jaffray, D. A. High solution gel-dosimetry by optical-CT and MR scanning. *Med. Phys.* **23**, 699–705 (2001).
30. Chuang, C. C. & Wu, J. Dose and slice thickness evaluation with nMAG gel dosimeters in computed tomography. *Sci. Rep.* **8**, 2632. <https://doi.org/10.1038/s41598-018-21022-8> (2018).
31. Chiu, C. Y., Tsang, Y. W. & Hsieh, B. T. N-isopropylacrylamide gel dosimeter to evaluate clinical photon beam characteristics. *Appl. Radiat. Isot.* **90**, 245–250. <https://doi.org/10.1016/j.apradiso.2014.04.015> (2014).
32. Mather, M. L. et al. Investigation of ultrasonic properties of PAG and MAGIC polymer gel dosimeters. *Phys. Med. Biol.* **47**, 4397–4409. <https://doi.org/10.1088/0031-9155/47/24/307> (2002).
33. Dorri Giv, M. et al. Characterization of improved PASSAG polymer gel dosimeter using magnetic resonance imaging. *Appl. Magn. Reson.* **53**, 441–455 (2022).
34. Vandecasteele, J. & De Deene, Y. On the validity of 3D polymer gel dosimetry: III. MRI-related error sources. *Phys. Med. Biol.* **58**, 63–85. <https://doi.org/10.1088/0031-9155/58/1/63> (2013).
35. Deene, Y. D. How to scan polymer gels with MRI? *J. Phys. Conf. S.* **250**. <https://doi.org/10.1088/1742-6596/250/1/012015> (2010).
36. Deene, Y. Chapter 9: gel-based radiation dosimetry using quantitative MRI. In: *NMR and MRI of Gels*. Royal Society of Chemistry, ISBN 978-1-78801-152-5, (2020).
37. Rabaeh, K. A. et al. Enhancements in 3D dosimetry measurement using polymer gel and MRI. *Radiat. Meas.* **43**, 1377–1382. <https://doi.org/10.1016/j.radmeas.2008.04.083> (2008).
38. Ibbott, G. S. et al. Three-dimensional visualization and measurement of conformal dose distributions using magnetic resonance imaging of BANG polymer gel dosimeters. *Int. J. Radiat. Oncol. Biol. Phys.* **38**, 1097–1103. [https://doi.org/10.1016/s0360-3016\(97\)00146-6](https://doi.org/10.1016/s0360-3016(97)00146-6) (1997).
39. Maryanski, M. J. et al. Magnetic resonance imaging of radiation dose distributions using a polymer-gel dosimeter. *Phys. Med. Biol.* **39**, 1437–1455. <https://doi.org/10.1088/0031-9155/39/9/010> (1994).
40. Farhood, B., Geraily, G. & Abtahi, S. M. M. A systematic review of clinical applications of polymer gel dosimeters in radiotherapy. *Appl. Radiat. Isot.* **143**, 47–59. <https://doi.org/10.1016/j.apradiso.2018.08.018> (2019).
41. Watanabe, Y. et al. Dose distribution verification in high-dose-rate brachytherapy using a highly sensitive normoxic N-vinylpyrrolidone polymer gel dosimeter. *Phys. Med.* **57**, 72–79. <https://doi.org/10.1016/j.ejmp.2018.12.007> (2019).
42. Furuta, T. et al. Comparison between Monte Carlo simulation and measurement with a 3D polymer gel dosimeter for dose distributions in biological samples. *Phys. Med. Biol.* **60**, 6531–6546. <https://doi.org/10.1088/0031-9155/60/16/6531> (2015).
43. Maryanski, M. J., Gore, J. C., Kennan, R. P. & Schulz, R. J. NMR relaxation enhancement in gels polymerized and cross-linked by ionizing radiation: a new approach to 3D dosimetry by MRI. *Magn. Reson. Imaging.* **11**, 253–258. [https://doi.org/10.1016/0730-725x\(93\)90030-h](https://doi.org/10.1016/0730-725x(93)90030-h) (1993).
44. De Deene, Y. Radiation dosimetry by use of radiosensitive hydrogels and polymers: mechanisms, state-of-the-art and perspective from 3D to 4D. *Gels* **8**, 599. <https://doi.org/10.3390/gels8090599> (2022).
45. Fong, P. M., Keil, D. C., Does, M. D. & Gore, J. C. Polymer gels for magnetic resonance imaging of radiation dose distributions at normal room atmosphere. *Phys. Med. Biol.* **46**, 3105–3113. <https://doi.org/10.1088/0031-9155/46/12/303> (2001).
46. Hayashi, S., Fujiwara, F., Usui, S. & Tominaga, T. Effect of inorganic salt on the dose sensitivity of polymer gel dosimeter. *Radiat. Phys. Chem.* **81**, 884–888. <https://doi.org/10.1016/j.radphyschem.2012.03.001> (2012).
47. Mattea, F., Chacón, D., Vedelago, J., Valente, M. & Strumia, M. C. Polymer gel dosimeter based on Itaconic acid. *Appl. Radiat. Isot.* **105**, 98–104. <https://doi.org/10.1016/j.apradiso.2015.07.042> (2015).

48. Jaszczak, M., Maras, P. & Kozicki, M. Characterization of a new N-vinylpyrrolidone-containing polymer gel dosimeter with pluronic F-127 gel matrix. *Radiat. Phys. Chem.* **177**, 109125. <https://doi.org/10.1016/j.radphyschem.2020.109125> (2020).
49. Rabaeh, K. A., Basfar, A. A., Almousa, A. A., Devic, S. & Mofiah, B. New normoxic N-(hydroxymethyl)acrylamide based polymer gel for 3D dosimetry in radiation therapy. *Phys. Med.* **33**, 121–126. <https://doi.org/10.1016/j.ejmp.2016.12.019> (2017).
50. Eyadeh, M. M., Smadi, S. A., Rabaeh, K. A., Oglat, A. A. & Diamond, K. R. Effect of lithium chloride inorganic salt on the performance of N-(Hydroxymethyl)acrylamide polymer-gel dosimeter in radiation therapy. *J. Radioanal. Nucl. Chem.* **330**, 1255–1261. <https://doi.org/10.1007/s10967-021-08036-9> (2021).
51. Rabaeh, K. A. et al. Substantial influence of magnesium chloride inorganic salt (MgCl<sub>2</sub>) on the polymer dosimeter containing N-(Hydroxymethyl)acrylamide for radiation therapy. *Results Phys.* **22**, 103862. <https://doi.org/10.1016/j.rinp.2021.103862> (2021b).
52. Rabaeh, K. A. et al. Improved performance of N-(Hydroxymethyl)acrylamide gel dosimeter using potassium chloride for radiotherapy. *Radiat. Meas.* **142**, 106542. <https://doi.org/10.1016/j.radmeas.2021.106542> (2021c).
53. Rabaeh, K. A. et al. Polymer gel containing N,N'-methylene-bis-acrylamide (BIS) as a single monomer for radiotherapy dosimetry. *Radiat. Phys. Chem.* **187**, 109522. <https://doi.org/10.1016/j.radphyschem.2021.109522> (2021a).
54. Rabaeh, K. A., Al-Tarawneh, R. E., Eyadeh, M. M., Hammoudeh, I. M. E. & Shatnawi, M. T. M. Improved dose response of N-(Hydroxymethyl)acrylamide gel dosimeter with calcium chloride for radiotherapy. *Gels* **8**, 78. <https://doi.org/10.3390/gels8020078> (2022).
55. Rabaeh, K. A. et al. Optical characterization of a new composition of acrylic acid hydrogel dosimeter for quality assurance in radiotherapy treatment. *J. Radioanal. Nucl. Chem.* **333**, 4873–4880. <https://doi.org/10.1007/s10967-024-09690-5> (2024).
56. Awad, S. et al. Utilizing acrylic acid polymer hydrogel for 3-D quality assurance in cyberknife radiotherapy. *Radiat. Phys. Chem.* **226**, 112300. <https://doi.org/10.1016/j.radphyschem.2024.112300> (2024).
57. Cheng, K. Y., Hsieh, L. L. & Shih, C. T. A comprehensive evaluation of NIPAM polymer gel dosimeters on three orthogonal planes and Temporal stability analysis. *PLOS ONE*, **11**, e0155797. <https://doi.org/10.1371/journal.pone.0155797> (2016).
58. Pourfallah, T. A. et al. Performance evaluation of MRI-based Pagat polymer gel dosimeter in an inhomogeneous Phantom using EGSNRC code on a co-60 machine. *Appl. Radiat. Isot.* **67**, 186–191. <https://doi.org/10.1016/j.apradiso.2008.09.006> (2009).
59. Rabaeh, K. A. & Eyadeh, M. M. Optical properties of polymerization N-(3-methoxypropyl) acrylamide polymer gel dosimeters for radiotherapy. *Pigm. Resin Technol.* **52** (2023), 755–760. <https://doi.org/10.1108/PRT-03-2022-0030> (2023).

## Acknowledgements

The authors would like to acknowledge the support of the Biomedical Physics Department, King Faisal Specialist Hospital and Research Center, Riyadh, Saudi Arabia under Project RAC#2240003.

## Author contributions

Belal Mofiah: Conceptualization, Methodology, Resources, Writing - Review & Editing, Supervision, Project administration. Khalid A. Rabaeh: Conceptualization, Methodology, Validation, Formal analysis, Investigation, Writing - Original Draft. Akram A. Moussa: Formal analysis, Investigation, Resources. Md Abdullah Al Kafi: Formal analysis, Investigation, Data Curation. Abdullah S. Bani Issa: Methodology, Investigation, Formal analysis.

## Funding

This research did not receive any specific grant from funding agencies in the public, commercial, or not-for-profit sectors.

## Declarations

## Competing interests

The authors declare no competing interests.

## Additional information

**Correspondence** and requests for materials should be addressed to B.M.

**Reprints and permissions information** is available at [www.nature.com/reprints](http://www.nature.com/reprints).

**Publisher's note** Springer Nature remains neutral with regard to jurisdictional claims in published maps and institutional affiliations.

**Open Access** This article is licensed under a Creative Commons Attribution-NonCommercial-NoDerivatives 4.0 International License, which permits any non-commercial use, sharing, distribution and reproduction in any medium or format, as long as you give appropriate credit to the original author(s) and the source, provide a link to the Creative Commons licence, and indicate if you modified the licensed material. You do not have permission under this licence to share adapted material derived from this article or parts of it. The images or other third party material in this article are included in the article's Creative Commons licence, unless indicated otherwise in a credit line to the material. If material is not included in the article's Creative Commons licence and your intended use is not permitted by statutory regulation or exceeds the permitted use, you will need to obtain permission directly from the copyright holder. To view a copy of this licence, visit <http://creativecommons.org/licenses/by-nc-nd/4.0/>.

© The Author(s) 2025